

# A study towards improving mechanical properties of sol–gel coatings for polycarbonate

Linda Y.L. Wu<sup>a,\*</sup>, Edmund Chwa<sup>b</sup>, Z. Chen<sup>b</sup>, X.T. Zeng<sup>a</sup>

<sup>a</sup> Singapore Institute of Manufacturing Technology, 71 Nanyang Drive, Singapore 638075, Singapore

<sup>b</sup> School of Materials Engineering, Nanyang Technological University, 50 Nanyang Avenue, Singapore 639798, Singapore

Received 22 September 2006; received in revised form 17 June 2007; accepted 19 June 2007

Available online 26 June 2007

## Abstract

Scratch-resistant coatings based on 3-glycidoxypolytrimethoxysilane and tetraethylorthosilicate with a cross-linking agent and different amounts of colloidal silica are prepared on polycarbonate substrates by sol–gel technique. The failure mode of this type of coating on soft plastic substrate under pencil scratch test is studied. It is found that the pencil scratch failure contains a gouge failure under the static pressure and a film cracking failure under the sliding of the pencil tip. The gouge failure is due to the early plastic deformation in the substrate, while the film cracking is due to the tensile stress in the film induced by the sliding and friction of the pencil tip. Factors influencing the static gouge failure and sliding cracking failure are investigated. It is found that the cross-linking agent and colloidal silica filler increase the intrinsic cross-linking, hardness, elastic modulus and fracture toughness of the coating material, therefore, reduce the film cracking tendency; whereas the increased layer thickness and multi-layer coating improve the pencil scratch resistance significantly via delayed plastic deformation in the substrate. Based on these analyses, we conclude that the main factors towards improved pencil scratch resistance are: layer thickness, elastic modulus, fracture toughness and intrinsic hardness of the coating material. Pencil hardness is increased from grade 2B to 5H by adjusting these parameters.

© 2007 Elsevier B.V. All rights reserved.

**Keywords:** Sol–gel; Coating; Scratch resistance; Hardness; Elastic modulus; Fracture toughness

## 1. Introduction

Transparent polymer materials (e.g. polycarbonate, PC) have been used to replace glasses and metals in a wide range of applications, such as display panels for hand-held electronic devices, compact disks, lightweight eyewear lenses and safety windows [1]. Despite their excellent physical and optical properties, the poor scratch and abrasion resistance has hindered their applications [2–5]. A hard and scratch-resistant protective coating is needed in order to improve the surface characteristics while capitalizing on their desirable bulk properties.

Organically modified silicate (also known as Ormosil) coatings have been extensively explored [6–11]. With the increasing applications in coating lenses [1,12], higher scratch resistance and durability on soft plastic for other protective applications (such as protective film for computer monitors) are required. The major

challenge for heavy loading scratch-resistant coatings is the too soft substrate, which deforms and causes coating's early failure even with a very hard thin coating. A good measure for coating's scratch resistance under heavy load is the pencil hardness, which can be tested by the ASTM standard D3363-00 [13] method and well accepted by the industry. With the increasing demands for higher scratch resistance and durable protective coatings for plastics, a good understanding on the pencil scratch failure mode and the major material properties influencing the pencil hardness is essential. The scratching damage of a thin coating on soft substrate under a pencil lead is a complex phenomenon. Boilot et al. [14] classified two categories of scratch behaviour: (1) fine scratches due to very small particles, (2) visible and wide cracks due to bigger particles. The latter is more related to the pencil scratch discussed in this paper. In this case, both substrate and coating properties contribute to the total scratch resistance. The ability of the coating to deform with the substrate is crucial. However, we have found that the failure mode under pencil scratching contains more than one failure mechanism, which needs a special study apart from the classical scratch mechanism.

\* Corresponding author. Tel.: +65 67938999; fax: +65 67916377.

E-mail address: [ylwu@simtech.a-star.edu.sg](mailto:ylwu@simtech.a-star.edu.sg) (L.Y.L. Wu).

This paper aims to analyse the failure mechanism under pencil scratching and study the influence of coating composition, the use of cross-linking agent and silica filler on the material's elastic modulus, fracture toughness, intrinsic hardness and the pencil grade. Although sol–gel coatings containing 3-glycidoxypropyl trimethoxysilane (GLYMO) and tetraethylorthosilicate (TEOS) and fillers have been reported [15–18], no direct analyses on failure mode of pencil scratching and the influencing factors towards pencil scratch resistance have been published.

## 2. Experimental details

### 2.1. Formulation of coating solutions

A stock solution of GLYMO-TEOS was prepared by hydrolysing them in ethanol (EtOH) and water (H<sub>2</sub>O) in an acidic solution (HIt, Itaconic acid). The molar ratios of the components were: GLYMO:TEOS:EtOH:H<sub>2</sub>O:HIt=1:1.63:2.19:5:0.26. The GLYMO and TEOS were hydrolysed separately and then mixed together. The mixture solution was stirred for 24 h and used as the base solution for coatings. To this base solution (A), a colloidal silica solution (Ludox AS-40) was first acidified by HIt to pH 3, and then added as hard filler in different molar ratios: 0.7, 2.08, 4.27 and 5.48. The colloidal silica was first coated with a monolayer of the sol–gel material by adding a small amount of solution A (15 wt.%). This was to stabilize the colloidal particles avoiding flocculation when added to the sol. After measuring the density of the cured un-filled coating (1.3 g/cm<sup>3</sup>), we calculated the volume percent of the filler in coating matrix, so that we have a better understanding of the filler distribution in the final coating layer. The above molar ratios of silica correspond to 6.7, 17.6, 30.5 and 36.0 vol.% in the cured coating matrix. Since the particle size of the silica is about 20 nm, the transparency of the coating was unaffected. Just before the dip coating process, 0.05 wt.% of ethylenediamine (ED) was added to the coating solution as the cross-linking agent of the epoxy ring in GLYMO.

### 2.2. Substrate preparation

Polycarbonate substrates, measured 100 mm × 50 mm × 3 mm, were supplied with a layer of protective film, which was peeled off before oxygen plasma treatment. The treatment was carried out just before the dip coating steps for all specimens used in the current work. The purpose for such a treatment is to remove organic contaminations on the PC surface and activate the surface for better wetting and adhesion between the coating and the substrate [19]. The treatment was done at the following conditions: radio frequency power 400 W; pressure 1.33 × 10<sup>4</sup> Pa; oxygen flow rate 400 cm<sup>3</sup>/min, and treatment time 5 min.

### 2.3. Coating and characterization

The pre-treated PC substrates were dip coated with the above solutions in different withdrawal speeds to study the effect of layer thickness on coating's hardness and scratch resistance. For thicker coatings (> 10 μm), 2 or 3 layers were applied. A curing step and a plasma treatment were carried out before the

subsequent layer was applied. This is to avoid merging of the two layers and cracking upon curing due to too much shrinkage. After the dip coating, specimens were placed in a bench top furnace for drying and curing. The drying was done at 80 °C for 40 min and curing at 110 °C for 90 min.

The thickness of the coating was measured using a profilometer (Talysurf Series 2 Stylus Profilometer) across the uncoated and coated areas on the same specimen. The adhesion between coating layer and substrate was assessed using the cross-cut tape test according to ASTM D 3359-02 [20] standard test method. The scratch resistance (termed as pencil hardness thereafter) of the coating was characterized by a commercial pencil hardness tester (Scratch Hardness Tester Model 291, ERICHSEN TESTING EQUIPMENT). The test conforms to ASTM Standard D3360-00 [13], where a vertical force of 7.5 ± 0.1 N was applied at 45° angle to the horizontal film surface as the pencil is moved over the coated specimen. Meanwhile the intrinsic hardness (referred to as nano-indentation hardness thereafter) and Young's modulus of the coatings were measured using a nano-indenter (NanoTest™). A Berkovitch tip (with a three-sided pyramid geometry) was employed. The load was controlled below 0.5 mN and the depth of the indentation was controlled to be less than 1/10 of the coating thickness in order to minimize the effect due to the substrate. The resultant displacement of the indenter into the surface is monitored with a sensitive capacitive transducer and displayed in real time as a function of load. The hardness and elastic modulus are then calculated by the established equations [21] by the software. To measure the film fracture toughness, coatings were applied on a PC thin substrate of 200 μm thick and tested by the controlled buckling test (tension) following our developed methods reported in [22–24]. Critical energy release rate,  $G_{IC}$ , was obtained as the measure of film toughness. The residual stress caused by curing shrinkage was calibrated in the calculation of the film toughness. The method to measure the residual stress is given in Ref. [25]. The chemical bonds in the coating layers were analysed by Fourier Transform Infrared Spectroscopy (FTIR, Bio-Rad Excalibur Series). Infrared absorption spectra of the coatings in the range of 4000–600 nm wavelengths were analysed by FTIR using the attenuated total reflectance (ATR, with Ge crystal) method. An infrared radiation is passed through an infrared transmitting crystal with a high refractive index, allowing the radiation to reflect within the ATR element several times. The absorption of radiation is related to fundamental vibrations of the chemical bonds, therefore, provides information related to the presence or absence of specific functional groups in the coatings.

## 3. Results and discussion

### 3.1. Effect of cross-linking agent

Coating solution B was prepared by adding a few drops (about 0.05 wt.%) of ethylenediamine (ED) to the base solution A (without colloidal silica filler). Ethylenediamine acts as an epoxy-curing agent, which opens the epoxy ring of GLYMO monomers and increases cross-linking density of the coating [6]. Fig. 1

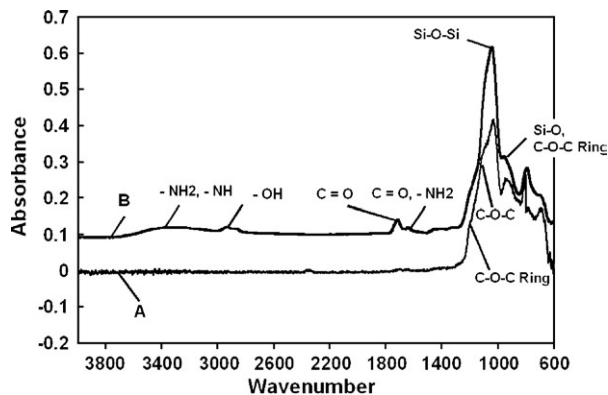


Fig. 1. FTIR spectra of coatings A and B, showing epoxy ring opening by the amine groups in the curing agent (ED).

shows the FTIR spectra of coatings from solution A and B. The additional peaks found on coating B (not on A) are:  $-NH$  and  $-NH_2$  groups at 3400 nm,  $C=O$  groups at 1600–1700 nm, and  $-OH$  groups at 2900 nm. All these groups, especially the  $C=O$  bond, indicate that the  $C-O-C$  rings in GLYMO have been opened and polymerization of GLYMO has occurred. Fig. 2 shows the diagram of epoxy ring opening. In the newly formed diol cross-linking [6,26], the two hydroxyl ( $-OH$ ) groups of the diol can form siloxane bonds with hydrolysed TEOS or GLYMO monomers through condensation. Therefore, cross-linking density will increase and a denser network structure, with intact organic groups dispersed throughout the network, can be formed. Nano-indentation, pencil hardness and thickness measurements of coating B were performed and the results were compared to that obtained from base coating A. Table 1 lists the results. It can be seen that coating B has 25% higher intrinsic hardness (0.59 GPa versus 0.47 GPa) than coating A. Both coatings provide improved pencil hardness (4–5 grades higher) for the soft substrate even with very thin layers. Coating B provides higher pencil hardness when layer thickness is increased above 4  $\mu\text{m}$ . Due to the higher cross-linking capability of solution B, thicker crack-free layer (4.9  $\mu\text{m}$ ) was formed at higher withdrawal speed, which is 70% thicker than the layer formed by solution A (2.9  $\mu\text{m}$ ). The higher intrinsic hardness by higher cross-linking density was also reported by several other authors [27,28].

Hardness is the resistance of a material to localized plastic deformation [29]. From an atomic perspective, plastic deformation corresponds to the breaking of bonds with original atom neighbours and then reforming new bonds as large numbers of atoms or molecules move relative to one another [30]. As such, the hardness of a material depends on the rigidity of its bonding

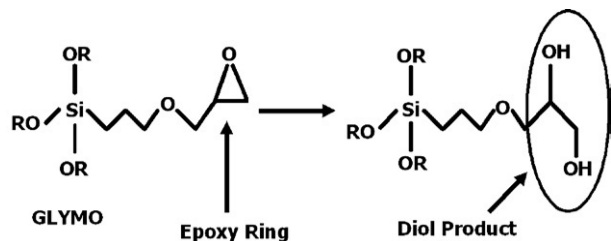


Fig. 2. Diol product from epoxy ring opening by ED.

Table 1

Pencil hardness, nano-indentation hardness, and film thickness of coatings A (base solution) and B (base solution with cross-linking agent)

Withdrawal speed (in/min)	Thickness ( $\mu\text{m}$ ) <sup>a</sup>		Pencil hardness		Hardness (GPa) <sup>a</sup>	
	A	B	A	B	A	B
PC substrate	0	0	6B	6B	–	–
10	2.0	2.3	2B	2B		
20	2.2	3.0	2B	2B		
25	2.5	3.5	2B	2B	0.47	0.59
30	2.6	4.7	2B	B		
35	2.9	4.9	2B	B		

There is no silica colloidal filler in these coatings.

<sup>a</sup> The standard deviation of indentation hardness is  $\pm 6\%$ , and thickness  $\pm 0.5 \mu\text{m}$ .

network. When cross-linking density in coating B increases, the rigidity of its bonding network increases due to additional  $\text{Si-O-Si}$  chains being joined together by the organic tail of the GLYMO monomers. This causes coating B to be more resistant to localized plastic deformation as it becomes more difficult for bonds to break and reform new bonds. Ethylenediamine was used in all the subsequent coatings prepared for this research.

### 3.2. Effect of silica filler

To further improve the mechanical properties of the coating, colloidal silica is used as the filler in different volume fractions. The surface of the colloidal filler contains hydroxyl groups that are pre-linked with a monolayer of GLYMO/TEOS to ensure good chemical bonding between the fillers and the matrix. The surface reactions are schematically shown in Fig. 3. The hydroxyl groups on particle surface react with the hydroxyl groups in hydrolysed GLYMO and TEOS to form  $\text{Si-O-Si}$  bond and further link with sol-gel matrix. Surface adsorption of GLYMO on silica colloidal was studied by Daniels and Francis [31], where the adsorption of GLYMO onto silica surface was evidenced by Nuclear Magnetic Resonance Spectroscopy. GLYMO was also used by other researchers [32] to modify the surface of  $\text{TiO}_2$  colloidal to enhance the stability of the colloidal in the hybrid sol-gel coating system. Fig. 4 shows the nano-indentation hardness, Young's modulus, the pencil hardness, and fracture toughness of the coatings with different

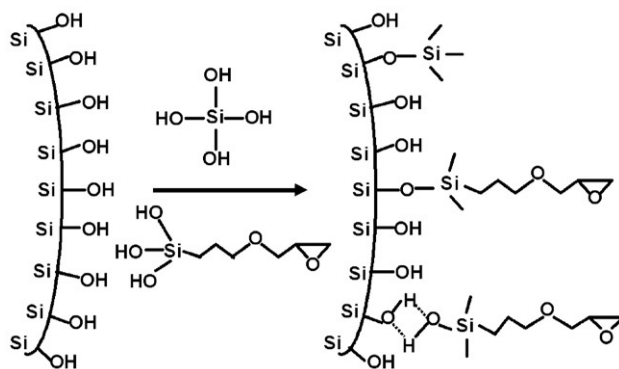


Fig. 3. Surface modification of colloidal silica for chemical bonding with sol-gel matrix.

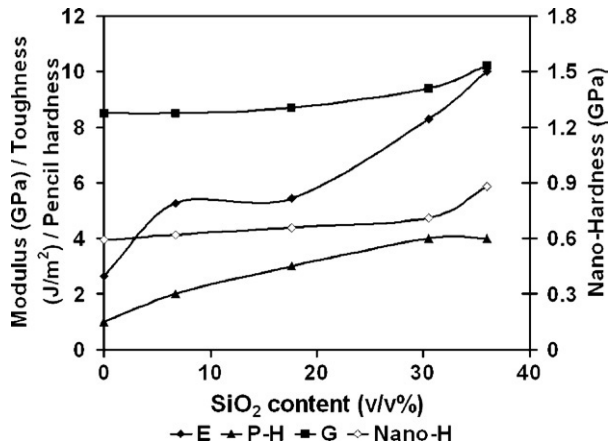


Fig. 4. Young's modulus ( $E$ ), pencil hardness ( $P-H$ ), toughness ( $G$ ) and Nano-indentation hardness (Nano-H) of coatings with different colloidal silica contents. (Pencil grades in this graph are indicative only. The actual grades for the points from low to high are: B, HB, F, H, 2H.). The standard deviation is  $\pm 6\%$  for nano-indentation hardness,  $\pm 6\%$  for  $E$ ,  $\pm 10\%$  for  $G$ , and  $\pm 20\%$  for  $P-H$ .

colloidal silica contents at the same coating thickness (within the range of  $5 \pm 0.5 \mu\text{m}$ ). As seen from the figure that elastic modulus has the most improvement (270%) with increasing silica content to 36 vol.%, followed by nano-indentation hardness (50%) and toughness (20%).

Pencil hardness shows continuous improvement to 3 higher grades with increasing silica content up to 30.5 vol.%, but remains stable till 36 vol.% silica content. The increase in hardness and elastic modulus was also reported by other researchers [30,33], which is due to the harder and stiffer matrix by the silica addition. No direct relation is found between pencil scratch grade and the ratio of intrinsic hardness or the elastic modulus. The increase in critical energy release rate caused by adding colloidal silica to the coating could be explained by the difference in porosity of the coatings before and after the colloidal silica is added. Coatings with colloidal silica added have a lower residual porosity due to the filling of the pores and the chemical bonding of the silica nano-particles with the sol-gel matrix. The pores in brittle films act as flaws causing stress concentration; and the larger the flaw size, the lower the film fracture resistance. Fig. 5 shows the fracture pattern under the

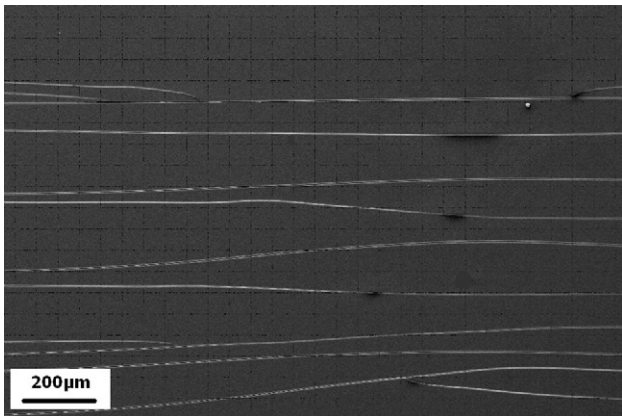


Fig. 5. SEM image of channelling cracks formed by buckling test (bending).

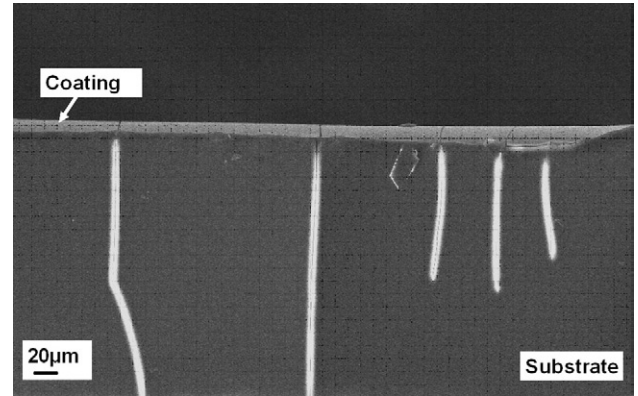


Fig. 6. Cross-section of the bent area showing cracks in both coating and substrate but no coating chip-off indicating good adhesion between coating and substrate.

buckling test, where the coating is subjected to bending. Parallel channelling cracks are observed, which is a typical failure pattern under tensile stress. When the localized tensile stress exceeded the critical tensile stress of the coating material, this kind of cracks formed. No coating chip-off is observed indicating good adhesion between the coating and the substrate. Fig. 6 shows the cross-section of the bent area. Cracks in both the coating and the substrate are observed, but no coating chip-off is observed. This indicates that the coating still conforms to the substrate at this high level of bending. The adhesion of the coatings was further confirmed by the cross-cut tape test. All the coatings showed excellent adhesion; no chip-off of coating at the edges of the crosscuts was observed.

### 3.3. Scratch failure mechanisms

A typical scratch failure pattern of the coating under pencil test is shown in Fig. 7. The failure contains an initial gouge under the static pressure and the very small contact area between the sharp pencil edge and the coated surface, and a cylindrical scratch mark under the sliding movement of the pencil lead. The gouge failure is related to the hardness of the

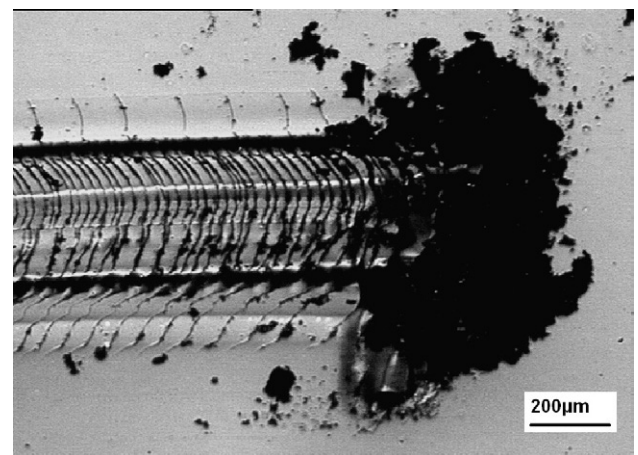


Fig. 7. Micrograph of a typical failure pattern of coating film after the pencil scratch test.

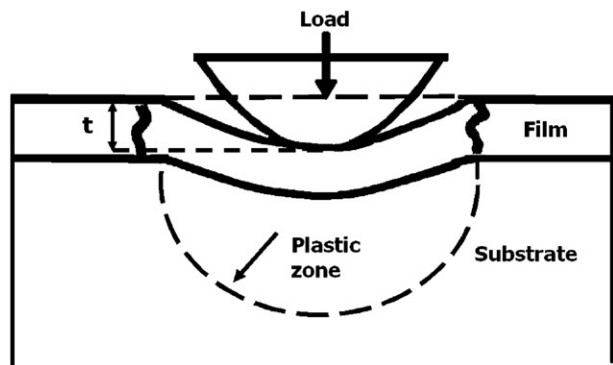


Fig. 8. Schematic diagram of gouge failure under the static pressure of pencil in the initial stage of pencil test.

coating as well as the strength of the substrate. The scratch mark shows micro-cracks both inside and outside of the mark. This indicates that the failure is by film cracking and substrate deformation. Fig. 8 shows a schematic diagram of gouge failure under the static pressure of pencil in the initial stage of pencil test. The coating is under tensile stress and the substrate undergoes a plastic deformation. When the pressure of the tip exceeds the yield strength of the substrate, a plastic deformation occurs and a gouge failure is formed on the coating surface.

Fig. 9 shows a schematic diagram of cracking damage under the sliding of pencil lead. With significant vertical loading applied, the substrate at the front edge may plastically deform and pileup. This could be well explained by the gouging mechanism discussed above. The coating behind the pencil lead (within the scratching mark) is also subjected to tensile stress due to friction. If this tensile stress exceeds the strength of the coating material, crack will form. During the formation of a scratch mark, the plastic deformation of substrate causes tensile stress in the coating layer outside but near the scratch mark, similar to the mechanism shown in Fig. 8. Therefore, cracks are also formed just outside the scratch mark. There was no clear sign of film delamination in the failure pattern, indicating that the adhesion between the coating and the substrate was strong enough. The higher coating toughness by silica filler helps to improve the pencil hardness via the delayed cracking under both the static pressure and the sliding movement of the pencil tip. Therefore, measuring the critical energy release rate, or fracture toughness, of the coating material could predict the coating's resistance to cracking and scratch failure. However,

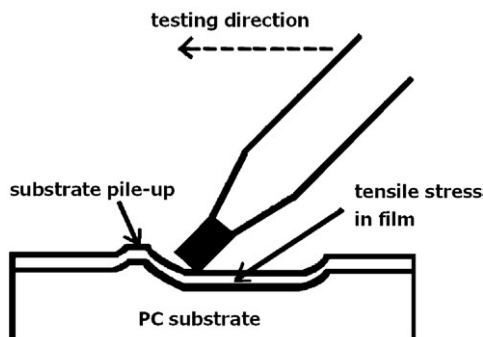


Fig. 9. Schematic illustration of cracking damage under the sliding of pencil lead.

fracture toughness is not the only factor in the scratch failure of a coating system. The effect of coating thickness is also very important, which will be addressed in the next section.

### 3.4. Effect of coating thickness on pencil hardness

Referring to the gouge failure mode described in Fig. 8, if the coating thickness ( $t$ ) could be increased to  $3t$ , the plastic zone would be within the coating material. In this case, since the yield strength of the coating material is much higher than the polycarbonate material, the maximum stress would not exceed the yield strength of the coating, therefore, no failure would occur. In our observations, the gouge failure is always followed by a crack failure due to that the pencil lead penetrates into the gouged area and an additional shear stress is introduced to the coating at the edge of the gouged area. When gouging occurs, the frictional force increases drastically. As a result the tensile stress in the trailing end increases, causing the ripple pattern as shown in Fig. 7. Therefore, it appears to be reasonable that in order to increase the pencil test grade, effort should be made to prevent the gouge failure first. In the current study, the coating thickness was varied from  $5.5 \mu\text{m}$  to  $25.1 \mu\text{m}$  by increasing withdrawal speed during dip coating and by double and triple layer coating. Fig. 10 shows the variation of pencil hardness grade with coating thickness. It's seen from the results that pencil hardness was much improved by thicker, double and triple coatings. This proves that thickening the coating is an effective way of improving the scratch resistance. This conclusion is only valid when the interfaces between any two layers are strong with good chemical bonding. Otherwise, the interfaces could become a weak zone causing early failure (either cracking or delamination) under the scratching condition. It is well known that a maximum crack-free layer thickness exists for each coating solution. Another condition for the above conclusion on the dependence of scratch hardness on layer thickness is that each coating layer is within the maximum crack-free layer thickness. The intrinsic hardness, being related to material properties, has no relation with coating thickness and remains approximately the same as thickness increases. This also proves that our coatings has consistent property throughout

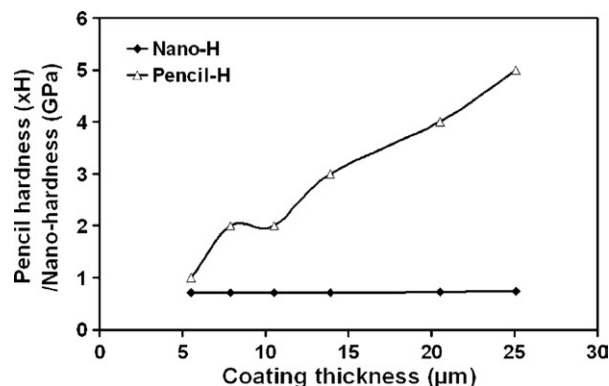


Fig. 10. Effect of coating thickness on pencil hardness grade and nano-indentation hardness. The standard deviation is  $\pm 6\%$  for nano-indentation hardness, and  $20\%$  for pencil hardness. The coating solution contains  $30.5 \text{ vol.}\%$  colloidal.

the layers, a good material network was formed, no matter thin layers or thick layers.

It should be mentioned that the pencil hardness is a rough test method, which can only be used to identify large enough differences. Pencil hardness grade remains the same within a few  $\mu\text{m}$  variation of thickness. With a thin coating of 5  $\mu\text{m}$  and below on the soft substrate, since it cannot withstand the initial pressure applied on the pencil lead, the improvement on pencil hardness is very limited.

### 3.5. Factors influencing scratch resistance in the sol–gel coatings

Based on the two mechanisms of pencil scratch failure, it is clear that besides the substrate factor, film cracking plays an important role in the scratch failure of the coating. In the current work we did not change the substrate material; therefore, the subsequent analysis will focus on the coating factors. From energy release point of view, cracking tendency is measured by the energy release rate,  $G$ , which is given by [34],

$$G = A_1 \frac{\sigma^2 t}{E} \quad (1)$$

where  $A_1$  is a factor related to the material system,  $\sigma$  the tensile stress,  $t$  the film thickness and  $E$  the elastic modulus of the film. In the case of gouging, the necessary condition is that the film will be bent till cracking occurs, so that the scratch object will be in touch with the substrate. The stress is related to the film bending due to contact loading:

$$\sigma = A_2 \frac{P}{t^2} \quad (2)$$

in which  $A_2$  is another factor related to material system,  $P$  is the vertical load transferred to the coating through the pencil tip. When the stress value ( $\sigma$ ) exceeds the critical tensile stress of the coating material, cracking failure will occur in the film. The stress related to this film cracking is inversely proportional to the square of the film thickness.

In the case of trailing edge, the tensile stress is proportional to the vertical load,  $P$ , and the friction coefficient,  $\mu$ , as in:

$$\sigma = A_3 \frac{\mu P}{bt} \quad (3)$$

where  $A_3$  is a factor related to material system, and  $b$  is the scratch width. The scratch width measured in Fig. 7 is approximately 250  $\mu\text{m}$ . Comparing Eq. (3) to Eq. (2), assuming the non-parametric factors  $A_2$  and  $A_3$  are comparable, since  $\mu$  is always below 1, and  $b$  is larger than  $t$ , the stress due to friction is always lower than the stress due to contact loading in our case. Since the load from pencil test is fixed to 7.5 N, the main factor that determines the film failure is the film thickness. This is in line with our experimental results (Fig. 10), where a 25  $\mu\text{m}$  thickness increased the pencil hardness by additional 4 grades comparing to a 5  $\mu\text{m}$  thick coating of the same coating material.

Combining Eqs. (1) and (2) or (1) and (3), it is clear that the scratch resistance is adversely affected by the load and the

friction coefficient, which agrees with the findings in other studies [35–37]. Meanwhile, it also points out that increasing film fracture toughness, elasticity modulus and thickness of the film helps to reduce the tendency of film cracking, and thus scratch failure. Mechanically, an increase in  $E$  and  $t$  increases both the bending and the tensile stiffness of the film; therefore the stress is reduced when other factors remain unchanged. In the range of parameters studied in the current work, increasing coating thickness has resulted in an improvement of 4 grades in the pencil hardness test (Fig. 10). Increasing silica addition improves the hardness, modulus and fracture toughness of the coating, and has resulted in an improvement of 3 pencil grades (Fig. 4).

It is worth mentioning that the above parametric analysis is based on the scratch test when film cracking is the dominant mode of failure. Further work is necessary for the other key mode of hard film failure by delamination. Once key parameters are identified, quantitative assessment on the effect of the key factors should be performed. Such analysis will help engineers in the design of scratch-resistant coatings.

## 4. Conclusion

Scratch-resistant coatings based on 3-glycidoxypropyltrimethoxysilane (GLYMO) and tetraethylorthosilicate (TEOS) with a cross-linking agent (ED) and different amounts of colloidal silica have been developed on polycarbonate substrates by sol–gel technique. The ED improved the intrinsic hardness of the coating material by 25%; and increased the crack-free layer thickness by 70%. Silica filler increased the elastic modulus by 270%, the nano-indentation hardness by 50%, and the fracture toughness by 20%. Since all these factors contribute to the pencil scratch resistance, the pencil hardness grade was increased by 4 grades on the same layer thickness of 5  $\mu\text{m}$ . It is further found that thicker and multi-layer coatings are very effective in improving the scratch resistance. A 25  $\mu\text{m}$  thickness increased the pencil hardness by additional 4 grades comparing to a 5  $\mu\text{m}$  thick coating of the same coating material. The failure mode under pencil scratch test consists of gouge failure under static pressure and film cracking under the sliding of pencil lead. A thicker layer reduces the stress transferred to the substrate and the coating, reducing the tendency of scratch failure. The analyses show that the major factors influencing pencil scratch resistance are substrate hardness/strength, coating thickness, elasticity modulus, fracture toughness and intrinsic hardness of the coating material. Pencil hardness was increased from grade 2B to 5H by adjusting these parameters.

## References

- [1] C. Charitidis, A. Laskarakis, S. Kassavetis, C. Gravalidis, S. Logothetidis, *Superlattices Microstruct.* 36 (2004) 171.
- [2] J.H. Lee, J.S. Cho, S.K. Koh, D. Kim, *Thin Solid Films* 449 (2003) 147.
- [3] D. Goutam, K. Debtosh, *J. Non-Cryst. Solids* 288 (2001) 221.
- [4] Y.B. Guo, C.N.F. Hong, *Diamond Relat. Mater.* 12 (2003) 946.
- [5] J.D. Mackenzie, E. Bescher, *J. Sol–Gel Sci. Technol.* 27 (2003) 7.
- [6] K.C. Song, J.K. Park, H.U. Kang, S.H. Kim, *J. Sol–Gel Sci. Technol.* 27 (2003) 53.

- [7] J.D. Wright, N.A.J.M. Sommerdijk, Sol–gel Materials Chemistry and Applications, Taylor & Francis Books Ltd, London, 2001.
- [8] C. Charitidis, M. Gioti, S. Logothetidis, S. Kassavetis, A. Laskarakis, I. Varsano, Surf. Coat. Technol. 357 (2004) 180.
- [9] T.P. Chou, G.Z. Cao, J. Sol–Gel Sci. Technol. 27 (2003) 31.
- [10] S.L. Man, J.J. Nam, J. Sol–Gel Sci. Technol. 24 (2002) 175.
- [11] G. De, D. Kundu, J. Non-Cryst. Solids 288 (2001) 221.
- [12] P. Barghoorn, U. Stebani, M. Balsam, Adv. Mater. 10 (1998) 635.
- [13] ASTM D3363-00, Standard Test Method for Film Hardness by Pencil Test, ASTM International, 2000.
- [14] J. Douce, J.-P. Boilot, J. Biteau, L. Scodellaro, A. Jimenez, Thin Solid Films 466 (2004) 114.
- [15] W. Tanglumlert, P. Prasassarakich, P. Supaphol, S. Wongkasemjit, Surf. Coat. Technol. 200 (2006) 2784.
- [16] P. Innocenzi, M. Esposto, A. Maddalena, J. Sol–Gel Sci. Technol. 20 (2001) 293.
- [17] S.R. Davis, A.R. Brough, A. Atkinson, J. Non-Cryst. Solids 315 (2003) 197.
- [18] A. Fidalgo, L.M. Ilharco, J. Non-Cryst. Solids 283 (2001) 144.
- [19] H.C. Ong, R.P.H. Chang, N. Baker, W.C. Oliver, Surf. Coat. Technol. 89 (1997) 38.
- [20] ASTM D3359-02, Standard Test Methods for Measuring Adhesion by Tape Test, ASTM International.
- [21] W.C. Oliver, G.M. Pharr, J. Mater. Res. 19 (2004) 3.
- [22] B. Cotterell, Z. Chen, Int. J. Fract. 104 (2000) 169.
- [23] Z. Chen, B. Cotterell, W. Wang, E. Guenther, S.J. Chua, Thin Solid Films 394 (2001) 202.
- [24] Z. Chen, B. Cotterell, W. Wang, Eng. Fract. Mech. 69 (2002) 597.
- [25] Z. Chen, X. Xu, C.C. Wong, S. Mhaisalkar, Surf. Coat. Technol. 167 (2003) 170.
- [26] T.L. Metroke, O. Kachurina, E.T. Knobbe, Prog. Org. Coat. 22 (2002) 295.
- [27] S. Wu, M.D. Soucek, Polymer 41 (2000) 2017.
- [28] S.S. Mahapatra, N. Karak, Prog. Org. Coat. 51 (2004) 103.
- [29] D. William, J. Callister, Materials Science and Engineering an Introduction, John Wiley & Sons, Inc, United States of America, 2003.
- [30] S. Pellice, P. Galliano, Y. Castro, A. Duran, J. Sol–Gel Sci. Technol. 28 (2003) 81.
- [31] M.W. Daniels, L.F. Francis, J. Colloid Interface Sci. 205 (1998) 191.
- [32] D.K. Hwang, J.H. Moon, Y.G. Shul, K.T. Jung, D.H. Kim, D.W. Lee, J. Sol–Gel Sci. Technol. 26 (2003) 783.
- [33] J. Malzbender, J.M.J. den Toonder, A.R. Balkenende, G. de With, Mater. Sci. Eng., R Rep. 36 (2002) 47.
- [34] J. Malzbender, G. de With, Surf. Coat. Technol. 135 (2001) 202.
- [35] M.H. Bless, G.B. Winkelman, A.R. Balkenende, J.M.J. den Toonder, Thin Solid Films 359 (2000) 1.
- [36] M.D.E. Coghill, D.H. Stjohn, Surf. Coat. Technol. 41 (1990) 135.
- [37] P.A. Steinman, Y. Tardy, H.E. Hintermann, Thin Solid Films 154 (1987) 333.